# Experimental investigations on the fatigue strength of welded joints on full-scale crane runway girders

Philipp Rettenmeier[1], Mathias Euler[2], Eberhard Roos[1], Ulrike Kuhlmann[2]

[1] Materials Testing Institute (MPA), University of Stuttgart,
Pfaffenwaldring 32, 70569 Stuttgart, Germany
Fax: 0711-685-63053, e-mail: philipp.rettenmeier@mpa.uni-stuttgart.de
[2] Institute of Structural Design, University of Stuttgart

***ABSTRACT.*** *Crane runways are steel structures cyclically stressed by wheel loads. These structures are usually realized by means of steel girders or beams with hot-rolled or plated I-sections and a block rail fastened by welding on the section's top flange. Due to the wheel loads the upper part of the girders including the rail welds is subjected to a local stress state mainly consisting of a local compression stress peak* $\sigma_{z,local}$ *and local shear stresses* $\tau_{xz,local}$*. Furthermore, this stress state is superimposed by welding residual stresses and normal and shear stresses as a consequence of global bending. Up to the present moment no systematical experimental investigation has been realised. A research project has been launched to investigate full-scale crane runways with welded rails in cyclic testing with stationary and reciprocating wheel loads to identify the contribution of damage on the multiaxiality. The paper solely focuses on the experimental investigations with reciprocating wheel loads. Especially the microstructural investigations on the location of the crack initiation and the development of the crack front are exemplified.*

## INTRODUCTION

Approximately 70% of crane runways for overhead travelling cranes consist of hot-rolled steel girders with fillet welded rails on top of the girder [1]. The described construction is schematically illustrated in Figure 1 a. In Figure 1 b the construction is depicted in a more detailed manner. Due to unavoidable tolerances there might be a void between the rail and the top flange's surface.

Figure 2 shows a crane runway girder that is subjected to a wheel load $F$ causing local compression $\sigma_{z,local}$ and local shear stresses $\tau_{xz,local}$. For reasons of simplification the global bending stresses $\sigma_x$ and $\tau_{xz}$ are not depicted as these stress components are small compared to the local stresses.

Considering the stress history of the cross-section of the girder in Figure 2 during a wheel passage it reveals that the occurring normal stresses and the shear stresses act out-of-phase and therefore cause a shift of the principal stress directions. Moreover, the applied stresses are superimposed by welding residual stresses induced by the

manufacturing process. Furthermore, three effects generate a stress concentration in crane runways according to [2]:

- material inhomogeneity due to the different material zones and grain sizes in the welded joint
- sharp notches in the weld toes and weld roots
- local stresses caused by the concentrated wheel load as described above

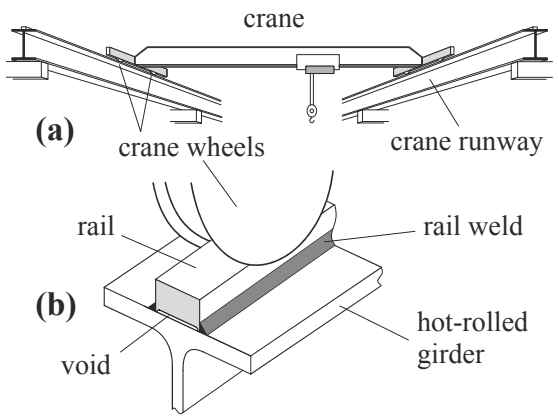


Figure 1. Travelling crane on crane runway (a) and crane runway construction (b)

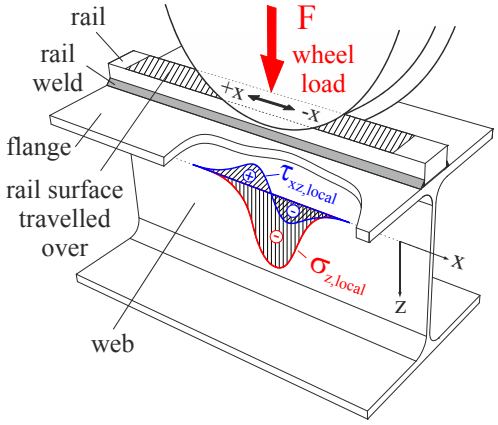


Figure 2. Schematic local stress state caused by a wheel load

The existing German Standard DIN 4132 [3] for crane runways compares the constructional details of the wheel load introduction with a cruciform joint under tensile loading. To account for the beneficial contribution of the compressive mean stress a bonus of 20 % on the fatigue strength is allowed.

Currently the fatigue part of the above mentioned national standard is replaced by the European Standard EN 1993-1-9 [4] that classifies several constructional details of the wheel load introduction more critically. Additionally a mean stress influence for welded structures in as-welded condition is excluded. As a consequence the allowable stress amplitudes drop by up to 33 % e.g. for cruciform joints with fillet welds [5]. Remarkably neither the German nor the European standard is able to refer to reliable test data for the constructional details of the wheel load introduction such as welded rails. The lower fatigue limits result in greater weld sizes or multipass welds. Up to the present moment there has not been a systematical experimental investigation of the fatigue behavior of the multiaxially stressed rail welds.

A research project has been launched to investigate the fatigue behavior of crane runways with welded rails. The achievable fatigue lives under stationary pulsating or reciprocating wheel loads with constant magnitude are determined in full-scale cyclic tests. In the following the first outcomes of the tests applying reciprocating wheel load are addressed. Especially the microstructural investigations on the location of the crack initiation and the development of the crack front are exemplified.

## EXPERIMENTAL INVESTIGATIONS

### *Test setup*

A total of ten single-span test girders are travelled over on the top rail surface by different wheel loads $F$ applied by a wheel block unit in combination with a vertical hydraulic cylinder, see Figure 3. The wheel block unit is commonly used in the crane industry. The wheel load is kept constant within each fatigue test.

The test girders are moved by a horizontal hydraulic cylinder in the test rig. The girder is travelled over on a length of $x = \pm 250$ mm. A frequency of 0.2 Hz per stress cycle is realized.

Though the wheel load is inteded to act centrically on the girder, small tolerances of the test specimens cause a slight amount of eccentricity that is exactly recorded by strain gauge measurements. No additional horizontal forces are applied.

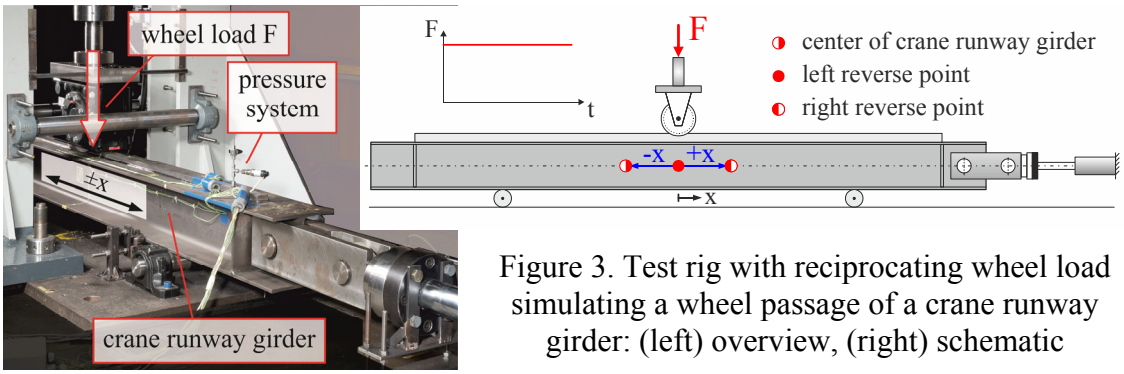


Figure 3. Test rig with reciprocating wheel load simulating a wheel passage of a crane runway girder: (left) overview, (right) schematic

### *Geometry and material properties of test specimens*

Both the hot-rolled girders with an I-section type HEA280 and the rectangular rails measuring 50 x 30 mm are fabricated by use of European mild steel S355J2+AR according to DIN EN 10025-2. The total length of the crane runway girders amounts to 3.5 m.

The chemical composition of both the rails and the girders is listed in Table 1. Additionally the base material properties both of the rails and the girders are taken from the material inspection certifications acc. to EN 10204, Sec. 3.1 and given in Table 2.

### *Fabrication and test procedure*

To ensure that the wheel load is only transferred from the rail into the top flange of the girder by the rail welds the rails were slightly recessed at the bottom side by milling. This procedure has been successfully established in a previos research project [5]. Subsequently the rail welds are simultaneously laid on both sides to the top flange of the girder by use of an automatically submerged welding process (welding reference number 121).

Table 1. Chemical composition of the base material (in weight %)

| *Material* | *C* | *Si* | *Mn* | *P* | *S* | *Cu* | *Cr* | *Ni* |
|---|---|---|---|---|---|---|---|---|
| Rail | 0.14 | 0.24 | 1.11 | 0.009 | 0.012 | 0.23 | 0.05 | 0.12 |
| Girder | 0.09 | 0.21 | 1.30 | 0.015 | 0.009 | 0.28 | 0.07 | 0.12 |

Table 2. Mechanical properties of the base material

| *Material* | *Yield strength* $R_e$ (MPa) | *Ultimate strength* $R_m$ (MPa) | *Elongation at fracture* $A_5$ (%) |
|---|---|---|---|
| Rail | 385 | 536 | 28 |
| Girder | 415 | 538 | 32 |

***Multiaxial load path caused by the wheel load***

The degree of non-proportionality of a stress history can be shown in a normal vs. shear strain diagram in which a diagonal represents in-phase loading and a circular path represents 90° out-of-phase loading [6], see Figure 4 a. The shear strain is generally divided by a factor of $\sqrt{3}$ or 2 depending on the applied equivalent strain criteria such as *Mises* or *Tresca*.

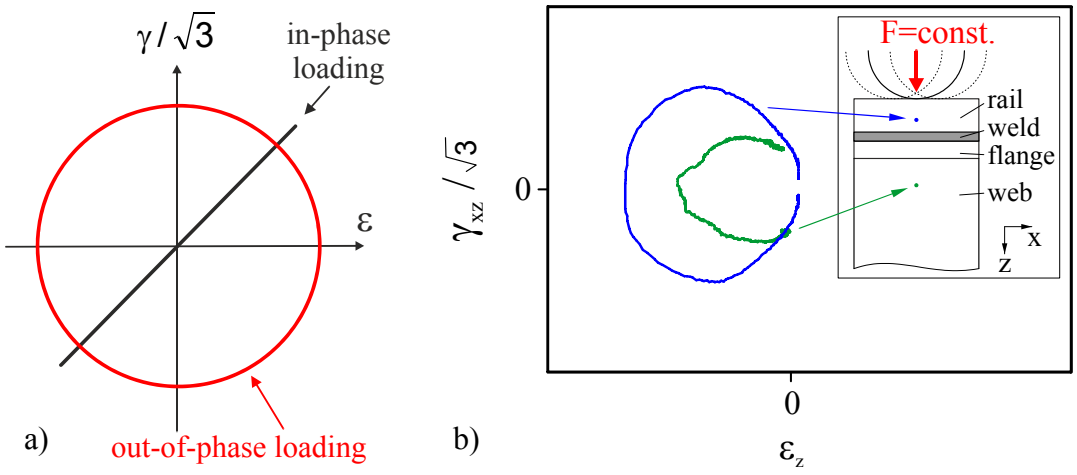


Figure 4. Multiaxial load path: (a) ideally in-phase and out-of-phase loading, (b) measured strain path during the passage of a wheel load *F*

During each fatigue test the strains in the girder's web are measured by strain gauges. For example the compression strain $\varepsilon_z$ and the shear strain $\gamma_{xz}$ are plotted in Figure 4 b for one wheel load level. Both measured strain paths are multiaxial and out-of-phase resulting in a complex fatigue stress state. The strain state for one particular material point on the rail's lateral surface (blue graph) is described by a closed circle as the rail is completely unloaded if the wheel is sufficiently removed from the location where the

strains are measured. Global shear strains in the rail are negligible. In contrast the circular path of the girder's web (green graph) cannot be closed since the web is subjected to significant global shear strains even though the wheel load is removed far away.

***Definition of failure criteria***

The rail welds show different failure mechanisms. Nevertheless, it seems that the major fatigue damage is caused by cracks initiated at the rail weld root. Several failure criteria were considered within the research project from those the following ones seem to be the most reasonable, also compare [7]:

- $N_1$: first through-thickness crack detected by a pressure system
- $N_2$: first crack observed by non-destructive testing (NDT)
- $N_3$: separation of the rail by complete longitudinal cracking of the weld

To determine the number of cycles $N_1$, the void between the rail and the girder is filled with air at a relative pressure of approximately 0.15 MPa before starting the tests. The pressure is chosen quite low in order to prevent any negative influence on the fatigue performance. For that reason a sensitive pressure system shown in Figure 3 is designed for a minimum pressure loss of $< 10^{-5}$ MPa/min. The magnitude of pressure is recorded together with the strain gauge data during the fatigue test by use of a data acquisition system. As soon as the first through-thickness crack of the rail welds appears the pressure drops immediately.

The number of cycles $N_2$ was determined by non-destructive testing (NDT) by permanent inspections. NDT starts after identification of the first through-thickness crack by the pressure system as described before. Afterwards the girder tests are stopped approximately every $10^4$ cycles for magnetic particle inspections using ultraviolet (UV) fluorescent spray and a UV light source.

Finally, the number of cycles $N_3$ to complete failure of the crane rail is reached when the rail is completely separated by crack propagation from the girder within the entire rail length travelled over by the wheel load.

## FIRST TEST RESULTS

The as-yet obtained results of the crane runway fatigue tests are summarized. In the following the test series was started with a maximum constant wheel load $F_{max}$. In the subsequent tests the wheel load $F$ was lowered. In the following a single passage of the wheel load from $-x$ to $+x$ or from $+x$ to $-x$ is referred to as one stress cycle, compare Figure 3.

In Figure 5 the magnitude of the wheel load $F$ in comparison to the maximum wheel load $F_{max}$ applied in the tests is plotted against the cycles to failure according to the different failure criteria described above. The number of cycles $N_1$ ranges between approximately 36'000 and 130'000 depending on the applied magnitude of the wheel load. Furthermore, it can be seen that the complete separation of the rail ($N_3$) takes place

significantly later at 117'000 to 900'000 cycles depending on the applied magnitude of wheel load. Figure 5 depicts forces instead of nominal stresses for the considered constructional detail "rail weld" as there has not been given an adequate nominal stress definition yet. A proposal for this definition will be developed in the near future within the ongoing research project. The test data for the crack initiation curve ($N_1$) in Figure 5 suggest a slope of about 3 that is characteristic for welded joints [8]. In contrast, the results for the curve of $N_3$ seem to exhibit a slightly shallower slope.

In Figure 6 the length of the crack propagation period is described. Herein the diagonal line indicates a critical failure without crack growth where the first through-thickness ($N_1$) crack is identical to the final failure ($N_3$) of the rail. For the tested crane runways the ratio of $N_3$ to $N_1$ amounts to 1.6 or higher indicating a significant crack propagation period.

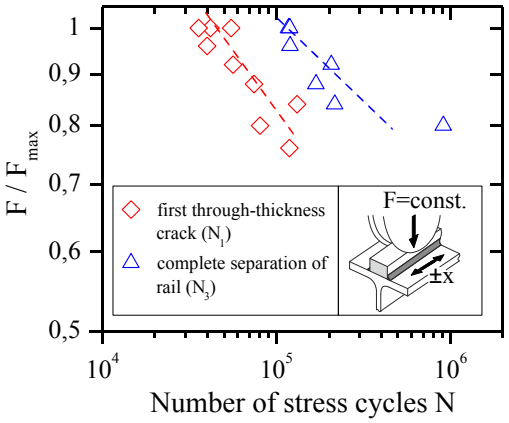


Figure 5. Experimental results in relation to the maximum wheel load $F_{max}$

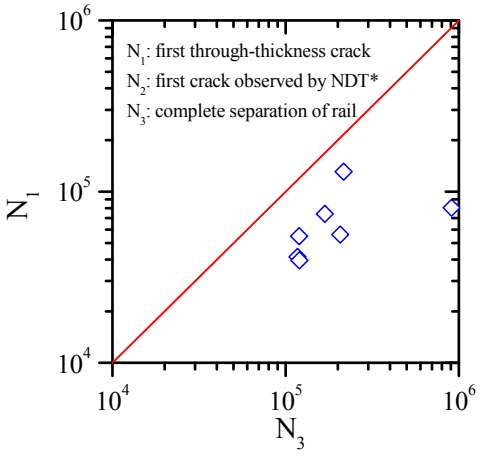


Figure 6. $N_1$ vs. $N_3$ (*NDT = nondestructive testing)

## CRACK PHANOMENA

Figure 7 shows the macrosection of a particular cross-section of a tested girder taken from the region travelled over by the wheel load. After sawing the cross-section is post-treated by etching ("Adler etch") to visualize the weld. In Figure 8 the deep weld penetration as a consequence of the submerged welding process and the void between the rail and top flange are clearly visible. Furthermore, Figure 8 indicates that cracks have been initiated at the weld root and the upper weld toe where the stress concentrations are extremely high. Moreover, plastic deformations of the rail's top surface can be recognized visually. Obviously crack propagation of the right weld has been already finalized in Figure 7, so that the welded joint of the rail is destroyed.

The stage of crack propagation of the left weld is shown in Figure 8. Three different cracks can be seen. Crack #1 initiated at the weld toe. Its propagation direction measures about 15° related to the y-direction. Remarkably the crack propagation is not

far advanced. In contrast, crack #2 exhibits a great crack growth and was obviously initiated at the weld root. The propagation direction at the early stage measures about 54°. Later the crack ran at an angle of approximately 24°. Finally, crack #3 also initiated at the weld root. In contrast to crack #2 this crack runs horizontally and its propagation rate is smaller. From the observed cracks crack #2 suggests to be the one being responsible for the through-thickness cracking of the rail weld.

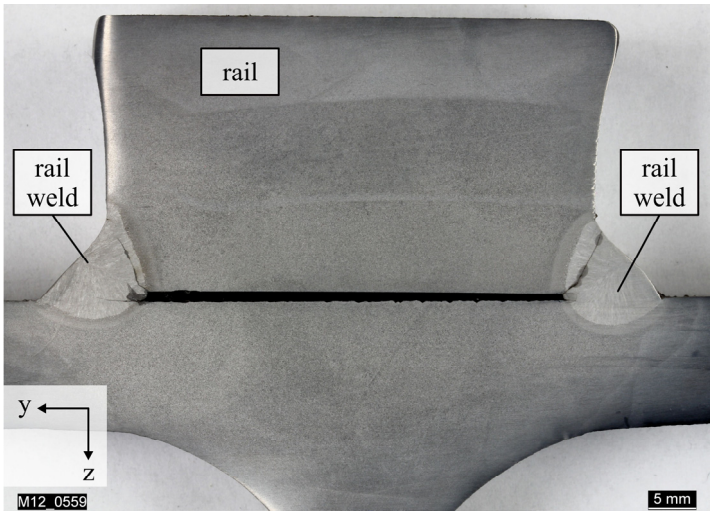


Figure 7. Macrosection of the crane runway

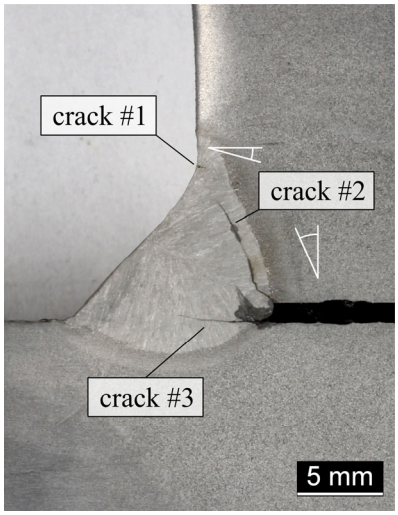


Figure 8. Detail of left weld

Figure 9 shows a longitudinal view of the cracking of the rail. The first through-thickness cracks appear close to the reverse points of the wheel load, see Figure 3. The cracks have got an arch-shaped form at an early crack growth stage suggesting that the shear stresses might be responsible for crack propagation.

In the center of the region travelled over by the wheel load the through-thickness cracking turns into a horizontally oriented straight crack that propagates in *x*-direction close to the lower weld toe, see Figure 10. In summary the crack phanomena are highly complex suggesting mixed mode crack propagation.

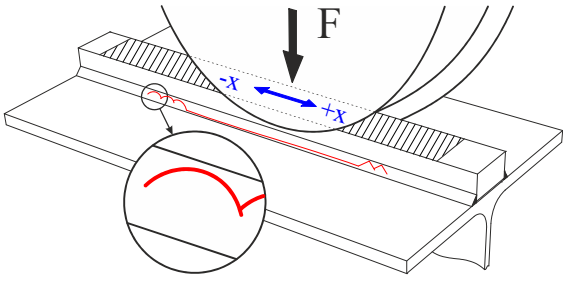


Figure 9. Propagated crack (exemplarily)

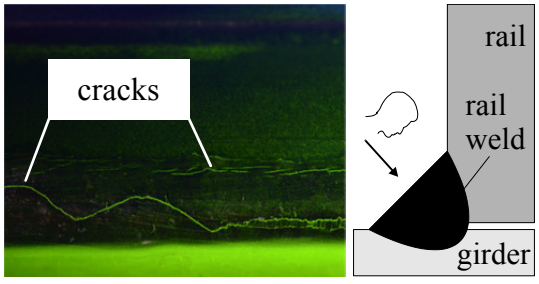


Figure 10. Weld cracks identified by NDT on surface of fillet weld along rail lengt

## CONCLUSIONS

Component tests of full-scale crane runway girders cyclically travelled over by a wheel load are performed in a comprehensive test rig. The following results are summarized:

- The local stress state of the crane runway due to the concentrated wheel load is multiaxial in nature. The measured strain paths during one load cycle indicates a non-proportional fatigue stressing of the crane runway girder.
- The experimental results are shown within the *S-N* curve for two failure criteria: at first through crack ("crack initiation") detected by a pressure system ($N_1$) and complete separation ("final failure") of the rail detected by non-destructive testing ($N_3$). The factor $N_3/N_1$ amounts at least 1.6 for the tested girders.
- The observed cracks caused by the cyclic wheel load suggest that both the local compression stress and the local shear stresses influence the crack initiation and crack propagation. The initiation of the cracks controlling the overall fatigue performance is suggested to take place at the weld root.

## ACKNOWLEDGEMENTS

The authors would like to acknowledge the DFG (Deutsche Forschungsgemeinschaft) for the financial support of the still ongoing research project „Ermüdungsverhalten von Stahlkonstruktionen unter multiaxialer Beanspruchung durch Radlasten" and the Goldbeck Group in Germany for sponsoring and fabricating the test girders.

## REFERENCES

1. Euler, M., Kuhlmann, U., (2011) *IJF*, **33**, pp. 1118-1126.
2. Radaj, D., Vormwald, M., (2007) *Ermüdungsfestigkeit – Grundlagen für Ingenieure*, p. 148, Springer Verlag Berlin, ISBN 978-3-540-71458-3 (in German)
3. DIN 4132, (1981) *Kranbahnen; Stahltragwerke*, Deutsches Institut für Normung (in German)
4. EN 1993-1-9, (2005) *Eurocode 3: Design of steel structures - Part 1-9: Fatigue*, European Committee for Standardization
5. Kuhlmann, U., Euler, M., (2007) *Wirtschaftliche Bemessung und Konstruktion robuster Radlasteinleitung*, IGF-Research Project No. 14173, Final Report, University of Stuttgart, Germany (in German)
6. Socie, D.F., Marquis, G.B., (2000) *Multiaxial Fatigue*, Society of Automotive Engineering R-234, Warrendale, ISBN 0-7680-0453-5
7. van Wirgende, A.M. van Delft, D.R.V., Wardenier, J. and Packer, J.A., (1997), *IIW Conference on Performance of Dynamically Loaded Welded Structures*, **50**, pp. 123-135
8. Radaj, D., Sonsino, C.M., Fricke, W., (2006) *Fatigue assessment of welded joints by local approaches*, 2nd edition, Woodhead Cambridge, ISBN 1-85573-948-8